IEEE Access
Multidisciplinary ⋮ Rapid Review ⋮ Open Access Journal

Received February 15, 2021, accepted February 22, 2021, date of publication February 24, 2021, date of current version March 4, 2021.

Digital Object Identifier 10.1109/ACCESS.2021.3061743

Coordination of a Flywheel Energy Storage Matrix System: An External Model Approach

HAIMING LIU, HUANLI GAO, SHUPING GUO, AND HE CAI, (Member, IEEE)
School of Automation Science and Engineering, South China University of Technology, Guangzhou 510641, China

Corresponding author: He Cai (caihe@scut.edu.cn)

This work was supported in part by the National Natural Science Foundation of China under Grant 61703167 and Grant 61803160, in part by the Guangdong Nature Science Foundation under Grant 2020A1515010810, in part by the Science and Technology Planning Project of Guangdong Province under Grant 2017A040405025, and in part by the Guangzhou Science Research Programme under Grant 201904010242.

ABSTRACT This paper studies the coordination of a heterogenous flywheel energy storage matrix system aiming at simultaneous reference power tracking and state-of-energy balancing. It is first revealed that this problem is solvable if and only if the state-of-energy of all the flywheel systems synchronize to a common time-varying manifold governed by a nonautonomous dynamic system. Next, by treating this nonautonomous dynamic system as an external model, the coordination problem can be decoupled into two separate problems, namely, the global double layer estimation problem and the local tracking problem. Then, a distributed control scheme is proposed to solve the coordination problem by integrating the adaptive distributed observer approach and the certainty equivalence control method. Comprehensive case studies are provided to show the performance of the proposed control scheme.

INDEX TERMS External model approach, flywheel energy storage matrix system, multiagent system.

I. INTRODUCTION

Flywheel energy storage system (FESS) is an important type of energy storage system which is indispensable to modern power system by maintaining balance between power supply and demand [1]–[4]. FESS stores energy as kinetic energy in the rotational mass of the flywheel, which has many feasible characteristics in contrast to other types of energy storage systems, such as high power and energy density, fast response, low maintenance and geographical free. Among all these characteristics, FESS generates no pollution, which makes it an environmental friendly way for the efficient and safe utilization of intermittent renewable energy.

So far, there have been extensive study on the control of a single FESS. In [5], the active disturbance rejection control techniques were adopted to improve the performance of the flywheel designed for DC microgrid applications. [6] considered the wide speed range operation for a FESS. A speed-dependent extended state observer was designed to realize global linearization, which together with an adaptive feedback control guaranteed consistent dynamic performance within the entire available operation range. In [7], by taking advantages of model predictive control, an optimal nonlinear controller was synthesized to deal with model uncertainties and external disturbances. In [8], an immersion and invariance manifold adaptive nonlinear controller for a constant DC-link voltage was proposed in the presence of the nonlinearity of the DC-link voltage in discharge and the fast discharge requirements of the FESS. On the other side, there has been less effort put into the coordination of a flywheel energy storage matrix system (FESMS), which consists of a group of flywheel systems to increase the power capacity and lower down the risk of single point failure [9]–[11]. Roughly speaking, the control schemes for the coordination of FESMS fall into two categories. The first one is the centralized control scheme, where the information of the entire FESMS should be known to all the subsystems. In [9], a power sharing mechanism was proposed in the way that the flywheel systems which stored the most energy have the priority to be put into use. While, this mechanism relies on the prerequisite that each flywheel system knows the energy levels of all the other flywheel systems and thus is centralized. Recently, motivated by the study on multiagent system, distributed control schemes have been introduced to the power society to deal with various problems. In distributed control scheme, each subsystem shall communicate with its neighboring

The associate editor coordinating the review of this manuscript and approving it for publication was Alexander Micallef.

subsystems over the communication network and thus less or even no global information will be needed. The communication network of the distributed control scheme can be made more sparse, and thus more economic competitive in contrast to that of the centralized control scheme which relies on all to all communication. Based on the average consensus algorithm, [10] proposed a distributed control scheme for the power sharing of a FESMS, where the sharing criterion is selected to be the current charging and discharging capacity. The work of [10] was later extended in [11] featuring periodic event-triggered and self-triggered control.

In general, there are two basic control objectives for an energy storage system. First, the power output of the entire energy storage system should follow its reference. Second, the energy level of each energy storage unit should be balanced to maintain the maximum power capacity of the entire energy storage system, since, otherwise, the energy storage units reaching critical high or low energy level will be forced offline, which would in turn cut down the power capacity of the entire energy storage system. For example, for battery energy storage systems, the state-of-charge should be balanced for all the battery cells/packs [12], [13], and for a general energy storage system, the state-of-charge can be generalized to the concept of state-of-energy (SOE), which is the ratio of the stored energy and the energy capacity [14], [15]. To the best of the author's knowledge, this paper for the first time considers the coordination problem of a heterogenous FESMS aiming at simultaneous reference power tracking and SOE balancing. It is first revealed that this problem is solvable if and only if the SOE of all the flywheel systems synchronize to a common time-varying manifold governed by a nonautonomous dynamic system. Next, by treating this nonautonomous dynamic system as an external model, the coordination problem can be decoupled into two separate problems, namely, the global double layer estimation problem and the local tracking problem. Then, a distributed control scheme is proposed to solve the coordination problem by integrating the adaptive distributed observer approach and the certainty equivalence control method. In contrast to the existing results, the novelties and main contributions of this paper are summarized as follows.

- In practice, there could be various criteria for power sharing under different application scenarios. In [10], [11], the criterion is the current charging and discharging capacity, and in this paper, the criterion is the SOE. Note that the current charging and discharging capacity is a static criterion, while the SOE is governed by a dynamic equation and thus is a dynamic criterion. As a result, the problem considered in this paper is more complex than those of [10], [11], and we need to precheck whether the solution to the power sharing problem exists or not based on the dynamic SOE criterion.
- In [10], [11], [14], no specific dynamics of the energy storage units were considered. While, in this paper, we have considered the specific rotor dynamics of the flywheel systems with heterogenous inertia, friction, and energy capacity parameters. In fact, the nonautonomous dynamic system which gives rise to the common time-varying manifold is depicted by all these parameters. In other words, these parameters implicitly determine how the reference power is shared among all the flywheel systems within the FESMS.
- In most of the existing results, say [9], [10], [12]–[15], the communication network is assumed to be static. In this paper, it is shown that the proposed control scheme is able to work under jointly connected communication network. Under the jointly connected assumption, the communication network can be disconnected for all time being as long as, from time to time, the union of these disconnected networks is connected. This feature endows the proposed control scheme with two advantages. On one hand, the proposed control scheme is embedded with certain robustness against unreliable communication environment resulted by either equipment fault or malicious attack. On the other hand, like [11], the information exchange within the FESMS can be cut down by predesign and thus the communication cost can be significantly reduced.

The above comparisons between the existing works and this work is summarized by Table 1. The rest of this paper is organized as follows. Notation adopted in this paper are summarized in Section II. Section III gives a mathematical problem formulation for the coordination problem. The main results of this paper are presented in Section IV, including the establishment of the sufficient and necessary condition for the solvability of the coordination problem, the design of the distributed control scheme, and the stability analysis of the closed-loop system. Case studies are shown in Section V, and the paper is concluded by Section VI.

II. NOTATION

$\mathbb{R}$ and $\mathbb{Z}^+$ denote the set of real numbers and positive integers, respectively. For $x_i \in \mathbb{R}^{n_i}$, $i = 1, \ldots, m$, $\mathrm{col}(x_1, \ldots, x_m) = [x_1^T, \ldots, x_m^T]^T$. $1_n = \mathrm{col}(1, \ldots, 1) \in \mathbb{R}^n$. For a matrix $A \in \mathbb{R}^{m\times n}$, $\mathrm{vec}(A) = \mathrm{col}(A_1, \ldots, A_n)$ where A_i is the ith column of A. $||x||$ denotes the Euclidean norm of a vector $x \in \mathbb{R}^n$ and $||A||$ denotes the Euclidean norm of a matrix $A \in \mathbb{R}^{m\times n}$. For a function $f(t) : [0, +\infty) \to \mathbb{R}^{m\times n}$, if there exist $p \in \mathbb{Z}^+$ and $\gamma_p, \ldots, \gamma_1, \gamma_0 \in \mathbb{R}$ such that

$$||f(t)|| \leq \gamma_p t^p + \cdots + \gamma_1 t + \gamma_0, \ \forall t \geq 0,$$

then $f(t)$ is said to be bounded by a polynomial function. $\otimes$ denotes the Kronecker product of matrices.

A graph $\mathcal{G} = (\mathcal{V}, \mathcal{E})$ consists of a node set $\mathcal{V} = \{1, \ldots, N\}$ and an edge set $\mathcal{E} \subseteq \mathcal{V} \times \mathcal{V}$. For $i, j = 1, 2, \ldots, N$, $i \neq j$, an edge of $\mathcal{E}$ from node i to node j is denoted by (i, j), and node i is called a neighbor of node j. Let $\mathcal{N}_i$ denote the set of all the neighbors of node i. If $\mathcal{G}$ contains a sequence of edges of the form $(i_1, i_2), (i_2, i_3), \ldots, (i_k, i_{k+1})$, then the set $\{(i_1, i_2), (i_2, i_3), \ldots, (i_k, i_{k+1})\}$ is called a path of $\mathcal{G}$ from node i_1 to node i_{k+1} and node i_{k+1} is said to be reachable from node i_1. A graph $\mathcal{G}$ is said to contain a spanning tree if there

TABLE 1. Comparisons between the existing works and this work.

	Existing Works	This Work
power sharing criteria	current charging/discharging capacity [10], [11]	SOE
energy storage unit dynamics	no specific dynamics [10], [11], [14]	flywheel dynamics
communication network	static and connected [9], [10], [12]–[15]	dynamic and jointly connected

exists a node in $\mathcal{G}$ such that all the other nodes are reachable from it, and this node is called the root of the spanning tree. Given a set of r graphs $\mathcal{G}_k = (\mathcal{V}, \mathcal{E}_k)$, $k = 1, \ldots, r$, the graph $\mathcal{G} = (\mathcal{V}, \mathcal{E})$ with $\mathcal{E} = \bigcup_{k=1}^{r} \mathcal{E}_k$ is called the union of $\mathcal{G}_k$ and is denoted by $\mathcal{G} = \bigcup_{k=1}^{r} \mathcal{G}_k$. A matrix $\mathcal{A} = [a_{ij}] \in \mathbb{R}^{N\times N}$ is said to be a weighted adjacency matrix of a graph $\mathcal{G}$ if

$$\begin{cases} a_{ii} = 0; \\ a_{ij} > 0 \Leftrightarrow (j, i) \in \mathcal{E}; \\ a_{ij} = 0 \Leftrightarrow (j, i) \notin \mathcal{E}. \end{cases}$$

Let $\mathcal{L} = [l_{ij}] \in \mathbb{R}^{N\times N}$ be such that

$$\begin{cases} l_{ii} = \sum_{j=1}^{N} a_{ij}; \\ l_{ij} = -a_{ij}, \qquad \text{if } i \neq j. \end{cases}$$

Then $\mathcal{L}$ is called the Laplacian of $\mathcal{G}$ associated with the weighted adjacency matrix $\mathcal{A}$. A time signal $\sigma(t)$: $[0, +\infty) \rightarrow \mathcal{P} = \{1, \ldots, n\}$ for some $n \in \mathbb{Z}^+$ is said to be a piecewise constant switching signal with dwell time τ for some $\tau > 0$ if there exists a time sequence $\{t_k, k \in \mathbb{Z}^+\}$ satisfying,

$$\begin{cases} t_0 = 0; \\ \forall k \in \mathbb{Z}^+,\ t_k - t_{k-1} \geq \tau; \\ \forall t \in [t_k, t_{k+1}),\ \sigma(t) = p,\ p \in \mathcal{P}. \end{cases}$$

Given a node set $\mathcal{V} = \{1, \ldots, N\}$ and a piecewise constant switching signal $\sigma(t)$, a switching graph can be defined as $\mathcal{G}_{\sigma(t)} = (\mathcal{V}, \mathcal{E}_{\sigma(t)})$ where $\mathcal{E}_{\sigma(t)} \subseteq \mathcal{V} \times \mathcal{V}$ for all $t \geq 0$. Let $\mathcal{A}_{\sigma(t)} = [a_{ij}(t)] \in \mathbb{R}^{N\times N}$ and $\mathcal{L}_{\sigma(t)} = [l_{ij}(t)] \in \mathbb{R}^{N\times N}$ denote the weighted adjacency matrix of $\mathcal{G}_{\sigma(t)}$ and the Laplacian of $\mathcal{G}_{\sigma(t)}$ associated with the weighted adjacency matrix $\mathcal{A}_{\sigma(t)}$, respectively. Moreover, let $\mathcal{N}_i(t)$ denote the set of all the neighbors of node i at time instant t.

III. PROBLEM FORMULATION

In this paper, we consider a FESMS consisting of N heterogenous flywheel systems, whose configuration is shown by Fig. 1. For $i = 1, \ldots, N$, the SOE dynamics[1] of the ith flywheel system are given by

$$\dot{\phi}_i(t) = -\frac{2B_{vi}}{I_i}\phi_i(t) - \frac{2\gamma_i}{I_i}P_{i,out}(t) \tag{1}$$

where $\phi_i(t)$, I_i, B_{vi} denote the SOE, inertia of the rotor, and friction coefficient, respectively, $\gamma_i = 1/\omega_{i\max}^2$ with $\omega_{i\max}$ denoting the maximum admissible angular velocity of the ith

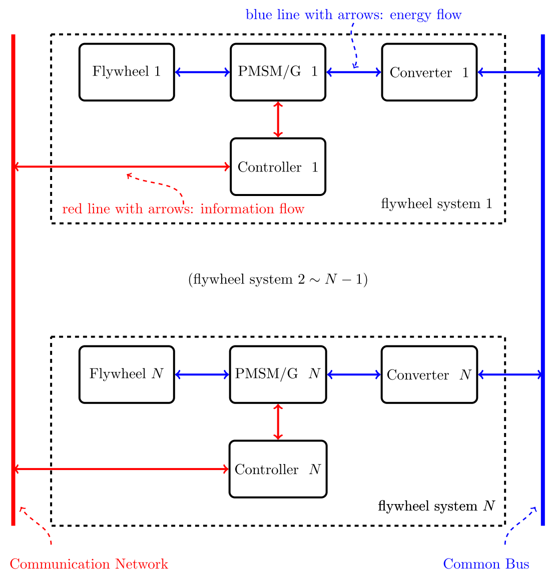

FIGURE 1. Configuration of the FESMS. (PMSM/G: permanent magnet synchronous motor/generator).

flywheel system, $P_{i,out}(t)$ denoting the net power output of the ith flywheel system is taken as the control input. Let

$$P_{FESMS}(t) = \sum_{i=1}^{N} P_{i,out}(t)$$

denote the power output of the entire FESMS, and $P_{REF}(t)$ denote the reference for $P_{FESMS}(t)$, which is assumed to be generated by a command generator in the following form

$$\dot{\eta}_0(t) = S_0\eta_0(t) \tag{2a}$$

$$P_{REF}(t) = C_0\eta_0(t) \tag{2b}$$

where $\eta_0(t) \in \mathbb{R}^q$ is the internal state of the command generator, $S_0 \in \mathbb{R}^{q\times q}$ and $C_0 \in \mathbb{R}^{1\times q}$ are constant matrices.

The communication network for the FESMS together with the command generator is modeled by a switching graph $\bar{\mathcal{G}}_{\sigma(t)} = (\bar{\mathcal{V}}, \bar{\mathcal{E}}_{\sigma(t)})$ with $\bar{\mathcal{V}} = \{0, 1, \ldots, N\}$ and $\bar{\mathcal{E}}_{\sigma(t)} \subseteq \{\bar{\mathcal{V}} \times \bar{\mathcal{V}}\}$. In here, the node 0 is associated with the command generator and the node i, $i = 1, \ldots, N$, is associated with the ith flywheel system of the FESMS. For $i = 0, 1, \ldots, N$, $j = 1, \ldots, N$, $(i, j) \in \bar{\mathcal{E}}_{\sigma(t)}$ if and only if the jth flywheel system can receive the information from the command generator if $i = 0$ or the ith flywheel system if $i \neq 0$ at time instant t. Let $\bar{\mathcal{A}}_{\sigma(t)} = \left[a_{ij}(t)\right] \in \mathbb{R}^{(N+1)\times(N+1)}$ be the weighted adjacency matrix of $\bar{\mathcal{G}}_{\sigma(t)}$, $\bar{\mathcal{L}}_{\sigma(t)}$ be the Laplacian of $\bar{\mathcal{G}}_{\sigma(t)}$ associated with the weighted adjacency matrix $\bar{\mathcal{A}}_{\sigma(t)}$, and $H_{\sigma(t)}$ consist of the last N row and the last N columns of $\bar{\mathcal{L}}_{\sigma(t)}$. The following assumption is imposed on the communication network.

[1] See APPENDIX A for the details of flywheel system modeling.

Assumption 1: There exists a subsequence $\{l_k : k = 0, 1, 2, \ldots\}$ of $\{k = 0, 1, 2, \ldots\}$ satisfying $t_{l_{k+1}} - t_{l_k} < \epsilon$ for some $\epsilon > 0$, such that every node i, $i = 1, \ldots, N$, is reachable from node 0 in the union digraph $\bigcup_{r=l_k}^{l_{k+1}-1} \mathcal{G}_{\sigma(t_r)}$.

Assumption 2: There is no time delay for the communication network $\mathcal{G}_{\sigma(t)}$.

Remark 1: In the literature of multiagent system, Assumption 1 is referred to as the "jointly connected" condition for a leader-follower multiagent system in many existing works, say [16], [17]. In contrast to the "spanning tree" condition for a static graph [12], [14], i.e., the communication graph is static and contains a spanning tree with node 0 as the root, and the "all time connected" condition for a switching graph [18], [19], i.e., the communication graph is switching and each subgraph should contain a spanning tree with node 0 as the root, the "jointly connected" condition imposes a much less restrictive requirement on the connectivity of the communication network. More specifically, the communication graph can be disconnected for all time being as long as, from time to time, the union of these disconnected graphs contains a spanning tree with node 0 as the root.[2] If a control scheme can work under Assumption 1, then it is endowed with at least two advantages. On one hand, the proposed control scheme is embedded with certain robustness against unreliable communication environment resulted by either equipment fault or malicious attack. On the other hand, the information exchange within the FESMS can be cut down by predesign and thus the communication cost can be significantly reduced.

Now, the coordination problem for the FESMS can be mathematically formulated as follows.

Problem 1: Given systems (1), (2) and the communication network $\bar{\mathcal{G}}_{\sigma(t)}$, design a distributed control scheme for $P_{i,out}(t)$, such that

$$\lim_{t\to\infty} (P_{FESMS}(t) - P_{REF}(t)) = 0, \tag{3}$$

and for $i, j = 1, \ldots, N$, $i \neq j$,

$$\lim_{t\to\infty} \left(\phi_i(t) - \phi_j(t)\right) = 0. \tag{4}$$

In what follows, the following assumption is made.

Assumption 3: The power output $P_{i,out}(t)$ is subject to no saturation constraint.

Remark 2: The control objective (3) requires that the power output of the entire FESMS should follow its reference, and the control objective (4) requires that the SOE of all the flywheel systems should be balanced. Our previous work [14] also considered these two control objectives for a general energy storage system. While, there are three major differences between [14] and this work. First, no specific dynamics were considered in [14] but simply the differential relationship between energy and power. On the contrary, in this work, we have considered the specific SOE dynamics of the flywheel system (1). Second, the communication network in [14] must be static and satisfy the spanning tree condition. In contrast, the communication network of this work can be jointly connected as described by Assumption 1. Third, the power reference $P_{REF}(t)$ in [14] was assumed to be a piecewise constant signal. While, in this work, $P_{REF}(t)$ is assumed to be generated by the command generator (2), which can accommodate a large class of reference signals as well as their combinations, such as step signals of arbitrary magnitudes, sinusoidal signals of arbitrary initial phases and amplitudes, and polynomial signals of arbitrary curve rates.

[2] See Fig. 4 of Section V for an example of "jointly connected" communication network.

IV. MAIN RESULTS

In this section, it is first proven that Problem 1 is solvable if and only if the SOE of all the flywheel systems synchronize to a common time-varying manifold governed by a nonautonomous dynamic system. Next, by treating this nonautonomous dynamic system as an external model, an augmented command generator is conceived which decouples the coordination problem into two separate problems, namely, the global double layer estimation problem and the local tracking problem. A distributed control scheme is then designed to solve Problem 1 under Assumption 1.

A. PROBLEM SOLVABILITY

Lemma 1: The following two equations simultaneously hold

$$P_{FESMS}(t) = P_{REF}(t) \tag{5a}$$

$$\phi_i(t) = \phi_j(t),\ i, j = 1, \ldots, N,\ i \neq j \tag{5b}$$

if and only if, for $i = 1, \ldots, N$, $\phi_i(t) = \psi_0(t)$, where $\psi_0(t)$ is governed by

$$\dot{\psi}_0(t) = -\alpha_0\psi_0(t) - \beta_0 P_{REF}(t) \tag{6}$$

with

$$\alpha_0 = \frac{2\sum_{i=1}^{N} \frac{B_{vi}}{\gamma_i}}{\sum_{j=1}^{N} \frac{I_i}{\gamma_i}},\ \beta_0 = \frac{2}{\sum_{i=1}^{N} \frac{I_i}{\gamma_i}}.$$

Proof: First, we show the "only if" part. (5b) implies

$$\dot{\phi}_i(t) - \dot{\phi}_j(t) = 0,\ i, j = 1, \ldots, N,\ i \neq j. \tag{7}$$

Then, by equations (1) and (7), for $i = 2, \ldots, N$, we have

$$\frac{2\gamma_1}{I_1}(P_{1,out}(t) + \frac{B_{v1}}{\gamma_1}\psi_0(t)) = \frac{2\gamma_i}{I_i}(P_{i,out}(t) + \frac{B_{vi}}{\gamma_i}\psi_0(t)). \tag{8}$$

Thus,

$$\begin{aligned} P_{i,out}(t) &= \frac{\gamma_1 I_i}{\gamma_i I_1}\left(P_{1,out}(t) + \frac{B_{v1}}{\gamma_1}\psi_0(t)\right) - \frac{B_{vi}}{\gamma_i}\psi_0(t) \\ &= \frac{\gamma_1 I_i}{\gamma_i I_1} P_{1,out}(t) + \left(\frac{B_{v1} I_i}{\gamma_i I_1} - \frac{B_{vi}}{\gamma_i}\right)\psi_0(t) \\ &= \frac{\gamma_1 I_i}{\gamma_i I_1} P_{1,out}(t) + \frac{B_{v1} I_i - B_{vi} I_1}{\gamma_i I_1}\psi_0(t). \end{aligned} \tag{9}$$

Therefore, by (5a), we have

$$\begin{aligned} P_{REF}(t) &= P_{FESMS}(t) \\ &= P_{1,out}(t) + \sum_{i=2}^{N} P_{i,out}(t) \end{aligned}$$

$$= P_{1,out}(t) + \sum_{i=2}^{N} \frac{\gamma_1 I_i}{\gamma_i I_1} P_{1,out}(t) + \sum_{i=2}^{N} \frac{B_{v1} I_i - B_{vi} I_1}{\gamma_i I_1} \psi_0(t)$$

$$= \sum_{i=1}^{N} \frac{\gamma_1 I_i}{\gamma_i I_1} P_{1,out}(t) + \sum_{i=2}^{N} \frac{B_{v1} I_i - B_{vi} I_1}{\gamma_i I_1} \psi_0(t). \quad (10)$$

By (5b), let $\psi_0(t) = \phi_i(t)$ for $i = 1, \ldots, N$, Then, by equation (1), we have

$$\dot{\psi}_0(t) = -\frac{2\gamma_i}{I_i}(P_{i,out}(t) + \frac{B_{vi}}{\gamma_i}\psi_0(t)). \quad (11)$$

Thus, we have

$$\dot{\psi}_0(t) = -\frac{2\gamma_1}{I_1}(P_{1,out}(t) + \frac{B_{v1}}{\gamma_1}\psi_0(t)). \quad (12)$$

Consequentially, substituting (10) into (12) gives

$$\begin{aligned}\dot{\psi}_0(t) &= -\frac{2\gamma_1}{I_1}\left(\frac{P_{REF}(t) - \sum_{i=2}^{N} \frac{B_{v1} I_i - B_{vi} I_1}{\gamma_i I_1}\psi_0(t)}{\sum_{i=1}^{N} \frac{\gamma_1 I_i}{\gamma_i I_1}} + \frac{B_{v1}}{\gamma_1}\psi_0(t)\right) \\ &= -\frac{2}{\sum_{i=1}^{N} \frac{I_i}{\gamma_i}} P_{REF}(t) + 2\left(\frac{\sum_{i=2}^{N} \frac{B_{v1} I_i - B_{vi} I_1}{\gamma_i I_1}}{\sum_{i=1}^{N} \frac{I_i}{\gamma_i}} - \frac{B_{v1}}{I_1}\right)\psi_0(t) \\ &= -\frac{2}{\sum_{i=1}^{N} \frac{I_i}{\gamma_i}} P_{REF}(t) + 2\frac{\sum_{i=2}^{N} \frac{B_{v1} I_i - B_{vi} I_1}{\gamma_i I_1} - \sum_{i=1}^{N} \frac{B_{v1} I_i}{I_1 \gamma_i}}{\sum_{i=1}^{N} \frac{I_i}{\gamma_i}}\psi_0(t) \\ &= -\frac{2\sum_{i=1}^{N} \frac{B_{vi}}{\gamma_i}}{\sum_{i=1}^{N} \frac{I_i}{\gamma_i}}\psi_0(t) - \frac{2}{\sum_{i=1}^{N} \frac{I_i}{\gamma_i}} P_{REF}(t). \quad (13)\end{aligned}$$

Next, we show the "if" part. Since all ϕ_i's are the same as (6), condition (5b) is satisfied immediately. Thus, we only need to show that condition (5a) is also satisfied. For $i = 1, \ldots, N$, it follows that

$$\begin{aligned}\dot{\phi}_i(t) &= -\frac{2B_{vi}}{I_i}\psi_0(t) - \frac{2\gamma_i}{I_i} P_{i,out}(t) \\ &= -\frac{2}{\sum_{i=1}^{N} \frac{I_i}{\gamma_i}} P_{REF}(t) - \frac{2\sum_{i=1}^{N} \frac{B_{vi}}{\gamma_i}}{\sum_{i=1}^{N} \frac{I_i}{\gamma_i}}\psi_0(t) \quad (14)\end{aligned}$$

and thus

$$P_{i,out}(t) = \frac{I_i}{\gamma_i}\left(\frac{1}{\sum_{i=1}^{N} \frac{I_i}{\gamma_i}} P_{REF}(t) + \frac{\sum_{i=1}^{N} \frac{B_{vi}}{\gamma_i}}{\sum_{i=1}^{N} \frac{I_i}{\gamma_i}}\psi_0(t) - \frac{B_{vi}}{I_i}\psi_0(t)\right). \quad (15)$$

As a result,

$$\begin{aligned}P_{FESMS}(t) &= \sum_{i=1}^{N} P_{i,out}(t) \\ &= \sum_{i=1}^{N} \frac{I_i}{\gamma_i}\left(\frac{1}{\sum_{i=1}^{N} \frac{I_i}{\gamma_i}} P_{REF}(t) + \frac{\sum_{i=1}^{N} \frac{B_{vi}}{\gamma_i}}{\sum_{i=1}^{N} \frac{I_i}{\gamma_i}}\psi_0(t) - \frac{B_{vi}}{I_i}\psi_0(t)\right) \\ &= \frac{\sum_{i=1}^{N} \frac{I_i}{\gamma_i}}{\sum_{i=1}^{N} \frac{I_i}{\gamma_i}} P_{REF}(t) + \frac{\left(\sum_{i=1}^{N} \frac{I_i}{\gamma_i}\right)\left(\sum_{i=1}^{N} \frac{B_{vi}}{\gamma_i}\right)}{\sum_{i=1}^{N} \frac{I_i}{\gamma_i}}\psi_0(t) - \sum_{i=1}^{N} \frac{B_{vi}}{\gamma_i}\psi_0(t) \\ &= P_{REF}(t). \quad (16)\end{aligned}$$

□

Remark 3: It can be seen that the nonautonomous dynamic system (6) is depicted by the parameters I_i, γ_i and B_{vi} of all the flywheel systems, and Lemma 1 together with (1) implicitly determines how the reference power shall be shared among all the flywheel systems within the FESMS.

B. CONTROL DESIGN

By treating the nonautonomous dynamic system (6) as an external model, an augmented command generator can be conceived by combining the nonautonomous dynamic system (6) and the command generator (2) as follows:

$$\dot{\eta}_0(t) = S_0 \eta_0(t) \quad (17a)$$
$$P_{REF}(t) = C_0 \eta_0(t) \quad (17b)$$
$$\dot{\psi}_0(t) = -\alpha_0 \psi_0(t) - \beta_0 P_{REF}(t). \quad (17c)$$

The augmented command generator (17) has a cascaded structure, i.e., the output $P_{REF}(t)$ of the command generator (17a)-(17b) is the input of the nonautonomous dynamic system (17c). This natural cascaded structure lends itself to the idea of decoupling the coordination problem into two separate problems, i.e., the global double layer estimation problem and the local tracking control problem. Then, for each flywheel system, an adaptive distributed observer, with the same cascaded double layer structure as (17), can be facilitated to estimate the common time-varying manifold governed by the nonautonomous dynamic system. Then, by further designing a local tracking controller which drives the local SOE to the common time-varying manifold, the problem will be solved by invoking Lemma 1.

For $i = 1, \ldots, N$, the control scheme for the ith flywheel system consists of the following three parts

1) the up-layer of command generator estimation

$$\dot{S}_i(t) = \mu_S \sum_{j=0}^{N} a_{ij}(t)(S_j(t) - S_i(t)) \tag{18a}$$

$$\dot{C}_i(t) = \mu_C \sum_{j=0}^{N} a_{ij}(t)(C_j(t) - C_i(t)) \tag{18b}$$

$$\dot{\eta}_i(t) = S_i(t)\eta_i(t) + \mu_\eta \sum_{j=0}^{N} a_{ij}(t)\left(\eta_j(t) - \eta_i(t)\right) \tag{18c}$$

$$\hat{P}_{i,REF}(t) = C_i(t)\eta_i(t) \tag{18d}$$

2) the down-layer of external model estimation

$$\dot{\alpha}_i(t) = \mu_\alpha \sum_{j=0}^{N} a_{ij}(t)(\alpha_j(t) - \alpha_i(t)) \tag{19a}$$

$$\dot{\beta}_i(t) = \mu_\beta \sum_{j=0}^{N} a_{ij}(t)(\beta_j(t) - \beta_i(t)) \tag{19b}$$

$$\begin{aligned}\dot{\psi}_i(t) &= -\alpha_i(t)\psi_i(t) - \beta_i(t)\hat{P}_{i,REF}(t)\\ &\quad + \mu_\psi \sum_{j=0}^{N} a_{ij}(t)(\psi_j(t) - \psi_i(t))\end{aligned} \tag{19c}$$

3) the local certainty equivalent tracking control

$$\begin{aligned}P_{i,out}(t) = -\frac{I_i}{2\gamma_i}\Big(&-\alpha_i(t)\psi_i(t) - \beta_i(t)\hat{P}_{i,REF}(t)\\ &- \kappa(\phi_i(t) - \psi_i(t)) + \frac{2B_{vi}}{I_i}\phi_i(t)\Big)\end{aligned} \tag{20}$$

where $S_i(t) \in \mathbb{R}^{q\times q}$, $C_i(t) \in \mathbb{R}^{1\times q}$, $\eta_i(t) \in \mathbb{R}^q$, $\hat{P}_{i,REF}(t), \alpha_i(t), \beta_i(t), \psi_i(t) \in \mathbb{R}$ are the estimates of S_0, C_0, $\eta_0(t)$, $P_{REF}(t)$, α_0, β_0 and $\psi_0(t)$, respectively.

The block diagram of the control scheme (18)-(20) is shown by Figs. 2 and 3, where Fig. 2 shows the block diagram of the global double layer estimation, and Fig. 3 shows the block diagram of the local tracking control. Systems (18a)-(18d) constitute the up-layer of command generator estimation to recover $P_{REF}(t)$, and systems (19a)-(19c) constitute the down-layer of external model estimation to recover $\psi_0(t)$. From Fig. 2, it can be seen that these two layers inherit the same cascaded structure as the augmented command generator (17). Systems (18) and (19) together constitute the estimator of the augmented command generator (17).

C. STABILITY ANALYSIS

Theorem 1: Given systems (1) and (17), under Assumption 1, if none of the eigenvalues of S_0 has positive real part, then the control scheme (18)-(20) solves Problem 1 for any $\mu_S, \mu_C, \mu_\eta, \mu_\alpha, \mu_\beta, \mu_\psi, \kappa > 0$.

Proof: For $i = 1, \ldots, N$, let $\bar{S}_i(t) = S_i(t) - S_0$, $\bar{C}_i(t) = C_i(t) - C_0$, $\bar{\alpha}_i(t) = \alpha_i(t) - \alpha_0$, $\bar{\beta}_i(t) = \beta_i(t) - \beta_0$, $\bar{S}(t) = \mathrm{col}(\bar{S}_1(t), \ldots, \bar{S}_N(t))$, $\bar{C}(t) = \mathrm{col}(\bar{C}_1(t), \ldots, \bar{C}_N(t))$, $\bar{\alpha}(t) = \mathrm{col}(\bar{\alpha}_1(t), \ldots, \bar{\alpha}_N(t))$, $\bar{\beta}(t) = \mathrm{col}(\bar{\beta}_1(t), \ldots, \bar{\beta}_N(t))$. Then it follows that

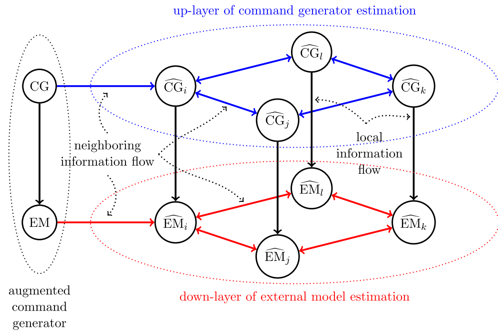

FIGURE 2. Block diagram of the global double layer estimation. (CG: command generator, EM: external model.)

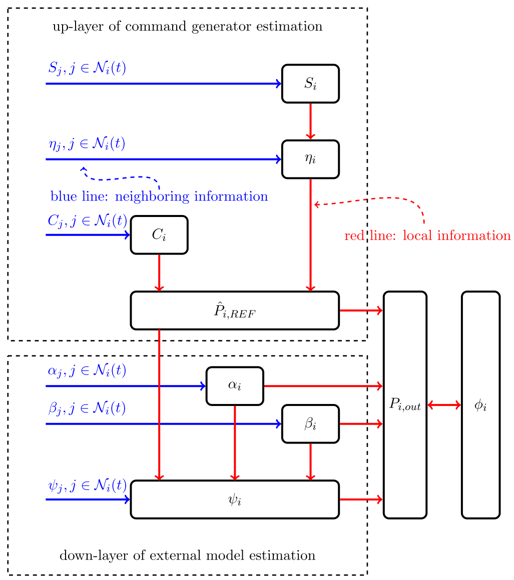

FIGURE 3. Block diagram of the local tracking control.

$$\mathrm{vec}(\dot{\bar{S}}(t)) = \mu_S(I_q \otimes H_{\sigma(t)} \otimes I_q)\mathrm{vec}(\bar{S}(t)) \tag{21a}$$

$$\mathrm{vec}(\dot{\bar{C}}(t)) = \mu_C(I_q \otimes H_{\sigma(t)})\mathrm{vec}(\bar{C}(t)) \tag{21b}$$

$$\dot{\bar{\alpha}}(t) = \mu_\alpha H_{\sigma(t)}\bar{\alpha}(t) \tag{21c}$$

$$\dot{\bar{\beta}}(t) = \mu_\beta H_{\sigma(t)}\bar{\beta}(t). \tag{21d}$$

By Corollary 4 of [17], it follows that all $\mathrm{vec}(\bar{S}(t))$, $\mathrm{vec}(\bar{C}(t))$, $\bar{\alpha}(t)$, $\bar{\beta}(t)$ will decay to zero exponentially as $t \to \infty$, i.e., all $\bar{S}_i(t), \bar{C}_i(t), \bar{\alpha}_i(t), \bar{\beta}_i(t)$ will decay to zero exponentially as $t \to \infty$. Meanwhile, all $S_i(t), C_i(t), \alpha_i(t), \beta_i(t)$ will be bounded for all $t \geq 0$.

For $i = 1 \ldots, N$, let $\bar{\eta}_i(t) = \eta_i(t) - \eta_0(t)$, $\bar{P}_{i,REF}(t) = \hat{P}_{i,REF}(t) - P_{REF}(t)$ and $\bar{\psi}_i(t) = \psi_i(t) - \psi_0(t)$. It follows that

$$\begin{aligned}\dot{\bar{\eta}}_i(t) &= S_i(t)\eta_i(t) + \mu_\eta \sum_{j=0}^{N} a_{ij}(t)\left(\eta_j(t) - \eta_i(t)\right) - S_0\eta_0(t)\\ &= S_i(t)\eta_i(t) + S_0\eta_i(t) - S_0\eta_i(t)\end{aligned}$$

$$\begin{aligned}
&+\mu_\eta \sum_{j=0}^{N} a_{ij}(t)\left(\bar{\eta}_j(t)-\bar{\eta}_i(t)\right)-S_0\eta_0(t)\\
&= S_0\bar{\eta}_i(t)+\bar{S}_i(t)\eta_i(t)+\mu_\eta \sum_{j=0}^{N} a_{ij}(t)\left(\bar{\eta}_j(t)-\bar{\eta}_i(t)\right)\\
&= S_0\bar{\eta}_i(t)+\bar{S}_i(t)\bar{\eta}_i(t)+\bar{S}_i(t)\eta_0(t)\\
&\quad+\mu_\eta \sum_{j=0}^{N} a_{ij}(t)\left(\bar{\eta}_j(t)-\bar{\eta}_i(t)\right) \qquad (22)
\end{aligned}$$

and

$$\begin{aligned}
\dot{\bar{\psi}}_i(t) &= -\alpha_i(t)\psi_i(t)-\beta_i(t)\hat{P}_{i,REF}(t)\\
&\quad+\mu_\psi \sum_{j=0}^{N} a_{ij}(t)(\psi_j(t)-\psi_i(t))\\
&\quad+\alpha_0\psi_0(t)+\beta_0 P_{REF}(t)\\
&= -\alpha_i(t)\psi_i(t)+\alpha_0\psi_i(t)-\alpha_0\psi_i(t)\\
&\quad-\beta_i(t)\hat{P}_{i,REF}(t)+\beta_i(t)P_{REF}(t)-\beta_i(t)P_{REF}(t)\\
&\quad+\mu_\psi \sum_{j=0}^{N} a_{ij}(t)(\psi_j(t)-\psi_i(t))\\
&\quad+\alpha_0\psi_0(t)+\beta_0 P_{REF}(t)\\
&= -\alpha_0\bar{\psi}_i(t)-\bar{\alpha}_i(t)\psi_i(t)-\bar{\beta}_i(t)P_{REF}(t)\\
&\quad-\beta_i(t)\bar{P}_{i,REF}(t)+\mu_\psi \sum_{j=0}^{N} a_{ij}(t)(\bar{\psi}_j(t)-\bar{\psi}_i(t))\\
&= -\alpha_0\bar{\psi}_i(t)-\bar{\alpha}_i(t)\bar{\psi}_i(t)-\bar{\alpha}_i(t)\psi_0(t)\\
&\quad-\bar{\beta}_i(t)P_{REF}(t)-\beta_i(t)\bar{P}_{i,REF}(t)\\
&\quad+\mu_\psi \sum_{j=0}^{N} a_{ij}(t)(\bar{\psi}_j(t)-\bar{\psi}_i(t)). \qquad (23)
\end{aligned}$$

Let $\bar{\eta}(t) = \mathrm{col}(\bar{\eta}_1(t),\ldots,\bar{\eta}_N(t))$ and $\bar{S}_d(t) = \text{block diag}\{\bar{S}_1(t),\ldots,\bar{S}_N(t)\}$. Then (22) can be written into the following compact form

$$\begin{aligned}
\dot{\bar{\eta}}(t) &= (I_N\otimes S_0-\mu_\eta(H_{\sigma(t)}\otimes I_q))\bar{\eta}(t)\\
&\quad+\bar{S}_d(t)\bar{\eta}(t)+\bar{S}_d(t)(1_N\otimes\eta_0(t)). \qquad (24)
\end{aligned}$$

By Corollary 1 of [16], it follows that $\lim_{t\to\infty}\bar{\eta}(t)=0$ exponentially. Since none of the eigenvalues of S_0 has positive real part, $\eta_0(t)$ and hence $P_{REF}(t)$ are bounded by polynomial functions. As a result, $\psi_0(t)$ is also bounded by a polynomial function since $\alpha_0>0$. Moreover,

$$\eta_i(t)=\bar{\eta}_i(t)+\eta_0(t)$$

implies that $\eta_i(t)$ is also bounded by a polynomial function since there exist $\rho_i, \varrho_i>0$ such that

$$||\bar{\eta}_i(t)|| \le \rho_i e^{-\varrho_i t} \le \rho_i$$

for all $t\ge 0$. Then, noting that

$$\bar{P}_{i,REF}(t)=C_i(t)\eta_i(t)-C_0\eta_0(t)=\bar{C}_i(t)\eta_i(t)+C_0\bar{\eta}_i(t)$$

and the fact that $\bar{C}_i(t)$ decays to zero exponentially gives that $\bar{P}_{i,REF}(t)$ decays to zero exponentially. Let $\bar{\psi}(t) = \mathrm{col}(\bar{\psi}_1(t),\ldots,\bar{\psi}_N(t))$, $\bar{\alpha}(t) = \mathrm{diag}\{\bar{\alpha}_1(t),\ldots,\bar{\alpha}_N(t)\}$, $\beta(t)=\mathrm{diag}\{\beta_1(t),\ldots,\beta_N(t)\}$, $\bar{\beta}(t)=\mathrm{diag}\{\bar{\beta}_1(t),\ldots,\bar{\beta}_N(t)\}$, and $\bar{P}_{REF}(t)=\mathrm{col}(\bar{P}_{1,REF}(t),\ldots,\bar{P}_{N,REF}(t))$. Then (23) can be written into the following compact form

$$\begin{aligned}
\dot{\bar{\psi}}(t) &= (-\alpha_0 I_N-\mu_\psi H_{\sigma(t)})\bar{\psi}(t)\\
&\quad-\bar{\alpha}(t)\bar{\psi}(t)-\bar{\alpha}(t)(1_N\otimes\psi_0(t))\\
&\quad-\bar{\beta}(t)(1_N\otimes P_{REF}(t))-\beta(t)\bar{P}_{REF}(t). \qquad (25)
\end{aligned}$$

Since $\bar{\alpha}(t), \bar{\beta}(t), \bar{P}_{REF}(t)$ decay to zero exponentially, $\beta(t)$ is bounded, and $\psi_0(t), P_{REF}(t)$ are bounded by polynomial functions, all $\bar{\alpha}(t)(1_N\otimes\psi_0(t))$, $\bar{\beta}(t)(1_N\otimes P_{REF}(t))$ and $\beta(t)\bar{P}_{REF}(t)$ decay to zero exponentially. Then, again by Corollary 1 of [16], it follows that $\lim_{t\to\infty}\bar{\psi}(t)=0$ exponentially. Then, similarly,

$$\psi_i(t)=\bar{\psi}_i(t)+\psi_0(t)$$

is bounded by a polynomial function.

Substituting (20) into (1) gives

$$\begin{aligned}
\dot{\phi}_i(t) &= -\frac{2B_{vi}}{I_i}\phi_i(t)-\frac{2\gamma_i}{I_i}\Big(-\frac{I_i}{2\gamma_i}[-\alpha_i(t)\psi_i(t)\\
&\quad-\beta_i(t)\hat{P}_{i,REF}(t)-\kappa(\phi_i(t)-\psi_i(t))+\frac{2B_{vi}}{I_i}\phi_i(t)]\Big)\\
&= -\alpha_i(t)\psi_i(t)-\beta_i(t)\hat{P}_{i,REF}(t)-\kappa(\phi_i(t)-\psi_i(t)). \qquad (26)
\end{aligned}$$

Let $\bar{\phi}_i(t)=\phi_i(t)-\psi_0(t)$. Then we have

$$\begin{aligned}
\dot{\bar{\phi}}_i(t) &= -\alpha_i(t)\psi_i(t)-\beta_i(t)\hat{P}_{i,REF}(t)-\kappa(\phi_i(t)-\psi_i(t))\\
&\quad+\alpha_0\psi_0(t)+\beta_0 P_{REF}(t)\\
&= -\kappa(\phi_i(t)-\psi_0(t)+\psi_0(t)-\psi_i(t))\\
&\quad-\alpha_0\bar{\psi}_i(t)-\bar{\alpha}_i(t)\psi_i(t)\\
&\quad-\bar{\beta}_i(t)P_{REF}(t)-\beta_i(t)\bar{P}_{i,REF}(t)\\
&= -\kappa\bar{\phi}_i(t)+\kappa\bar{\psi}_i(t)-\alpha_0\bar{\psi}_i(t)-\bar{\alpha}_i(t)\psi_i\\
&\quad-\bar{\beta}_i(t)P_{REF}(t)-\beta_i(t)\bar{P}_{i,REF}(t). \qquad (27)
\end{aligned}$$

Since $\bar{\alpha}_i(t), \bar{\beta}_i(t), \bar{P}_{i,REF}(t), \bar{\psi}_i(t)$ decay to zero exponentially, $\beta_i(t)$ is bounded, and $\psi_i(t), P_{REF}(t)$ are bounded by polynomial functions, all $\kappa\bar{\psi}_i(t)$, $\alpha_0\bar{\psi}_i(t)$, $\bar{\alpha}_i(t)\psi_i(t)$, $\bar{\beta}_i(t)P_{REF}(t)$, $\beta_i(t)\bar{P}_{i,REF}(t)$ will decay to zero exponentially. Then, since $\kappa>0$, $\lim_{t\to\infty}\bar{\phi}_i(t)=0$, and thus the proof is completed by invoking Lemma 1. □

Remark 4: Assuming none of the eigenvalues of S_0 has positive real part merely rules out exponentially increasing signals, which are barely used in practice since the increasing rate of exponential functions is too fast.

Remark 5: As is often the case, over the communication network, the time response of the node near the command generator will be faster than that of the node far away from the command generator. As a result, when the number of the nodes increases, it would probably take longer time for the system to settle down. A possible solution to this problem could be an elegant design of the communication network topology such that most of the nodes are within certain range of the command generator.

TABLE 2. System friction, inertia and energy capacity parameters.

	B_{vi}	$I_i(\mathrm{kg}\cdot\mathrm{m}^2)$	$\omega_{i,\max}(\mathrm{rad/s})$
1	1×10^{-3}	0.8	1000
2	0.95×10^{-3}	0.9	800
3	1.05×10^{-3}	1.0	900
4	0.9×10^{-3}	1.3	1200

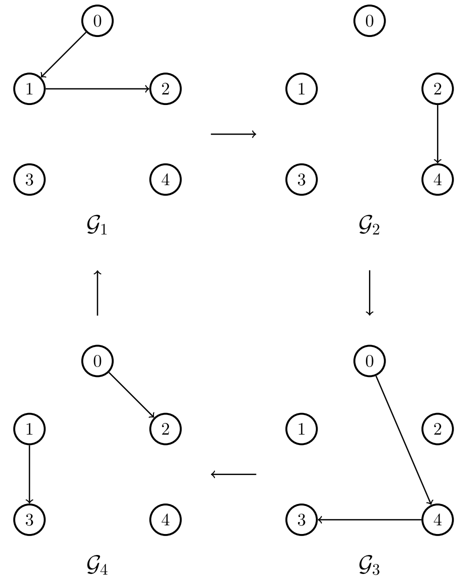

FIGURE 4. Communication network $\mathcal{G}_{\sigma(t)}$ switches periodically among $\mathcal{G}_1$, $\mathcal{G}_2$, $\mathcal{G}_3$, and $\mathcal{G}_4$.

V. CASE STUDIES

In this section, we consider a FESMS consisting of four flywheel systems. The communication network is shown by Fig. 4 where $\mathcal{G}_{\sigma(t)}$ switches among four graphs $\mathcal{G}_1$, $\mathcal{G}_2$, $\mathcal{G}_3$, and $\mathcal{G}_4$ periodically. Suppose the period is T_ps. It can be seen that all these four graphs are disconnected, while the union of them contains a spanning tree with node 0 as the root, and thus Assumption 1 is satisfied. The system parameters are given by Table 2. The command generator is designed as

$$\begin{aligned} \dot{\eta}_0(t) &= \begin{pmatrix} 0 & 0.1 \\ -0.1 & 0 \end{pmatrix} \eta_0(t) \\ P_{REF}(t) &= \begin{pmatrix} 1 & 0 \end{pmatrix} \eta_0(t) \\ \eta_0(0) &= \begin{pmatrix} 0 \\ 2\times10^5 \end{pmatrix}. \end{aligned} \tag{28}$$

Thus, $P_{REF}(t) = 20\sin(0.1\ t)$ kw. In what follows, we will consider a series of case studies to examine the performance of the proposed control scheme under different scenarios.

A. STANDARD CASE

In this case, we let $T_p = 1$s. The control gains are selected to be $\mu_S = \mu_C = \mu_\eta = \mu_\alpha = \mu_\beta = \mu_\psi = 100$, $\kappa = 1$. The system initial values are given by $\psi_0(0) = 0.88$, $\phi_1(0) = \psi_1(0) = 0.85$, $\phi_2(0) = \psi_2(0) = 0.9$, $\phi_3(0) = \psi_3(0) = 0.88$, $\phi_4(0) = \psi_4(0) = 0.87$, and for $i = 1, 2, 3, 4$, $S_i(0) = 0$, $C_i(0) = 0$, $\eta_i(0) = 0$, $\alpha_i(0) = 0$, $\beta_i(0) = 0$. The system performance is shown by Fig. 5. It can be seen that both SOE balancing and power tracking have been successfully achieved.

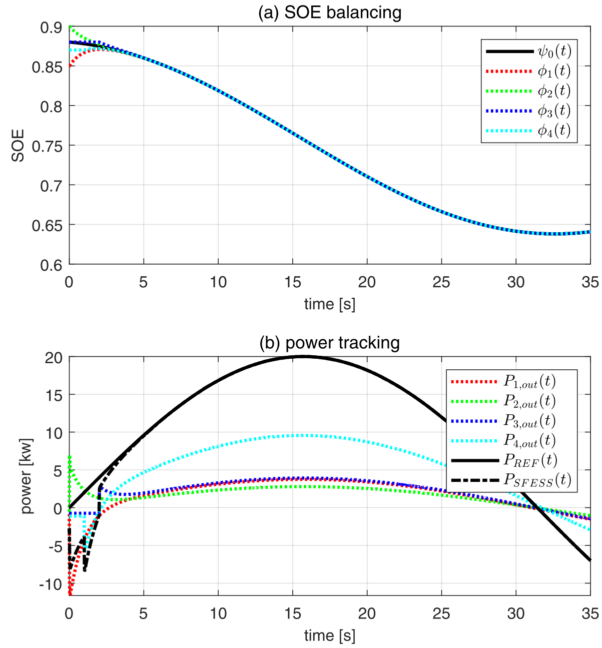

FIGURE 5. System performance for the standard case.

B. EFFECT OF THE POWER LOSS ON SYSTEM PERFORMANCE

The power loss of the FESMS mainly comes from two sources: the self-loss of the flywheels due to friction and the loss on transmission lines. As can be seen in Appendix A, the self-loss of the flywheels is taken into consideration in the flywheel modeling and thus has been compensated by the proposed control scheme. On the other side, in this paper, the reference power $P_{REF}(t)$ for the FESMS is determined by the command generator (2), which is an autonomous system taking no feedback from the actual power output $P_{FESMS}(t)$ of the FESMS. As a result, the power loss on transmission lines cannot be compensated autonomously by the proposed control scheme, but probably by pre-increasing the reference power. For the case of 10% power loss on transmission lines, the system performance is shown by Fig. 6. While, if the FESMS is spatially concentrated as assumed in [20], then the power loss on transmission lines shall be neglectable. Nevertheless, it seems feasible to achieve autonomous power loss compensation by combining the proposed control scheme and the control scheme of [14], and this will be considered as our future work.

C. EFFECT OF THE INTERMITTENCY OF THE SWITCHING COMMUNICATION NETWORK ON SYSTEM PERFORMANCE

In this case, we check the effect of the intermittency of the switching communication network on system performance. In contrast to the standard case, we test the scenarios where $T_p = 0.1$s and $T_p = 2$s, respectively. The simulation results are shown by Figs. 7 and 8,

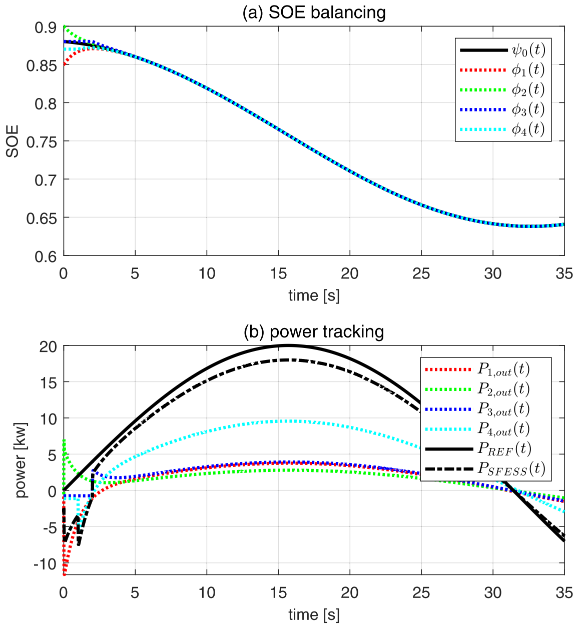

FIGURE 6. System performance for the case of 10% power loss on transmission lines.

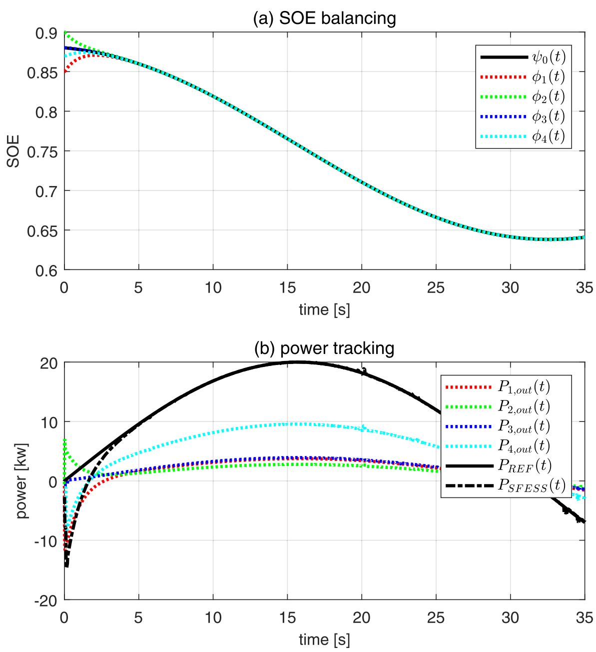

FIGURE 7. System performance for the case of $T_p = 0.1$s.

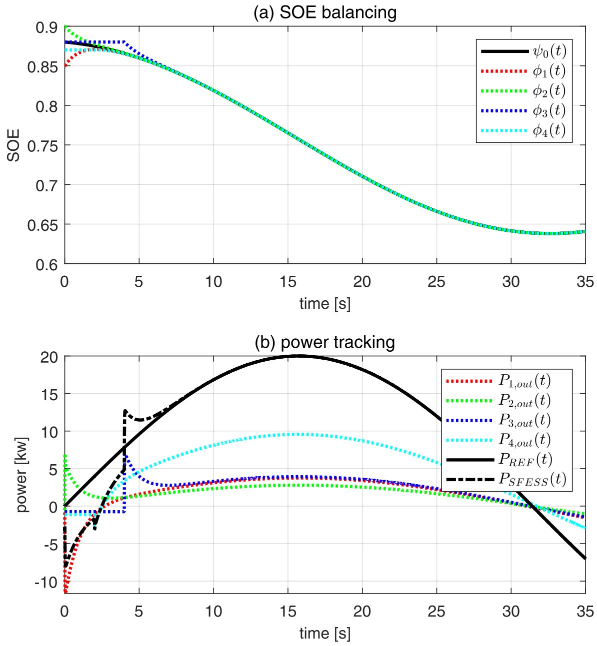

FIGURE 8. System performance for the case of $T_p = 2$s.

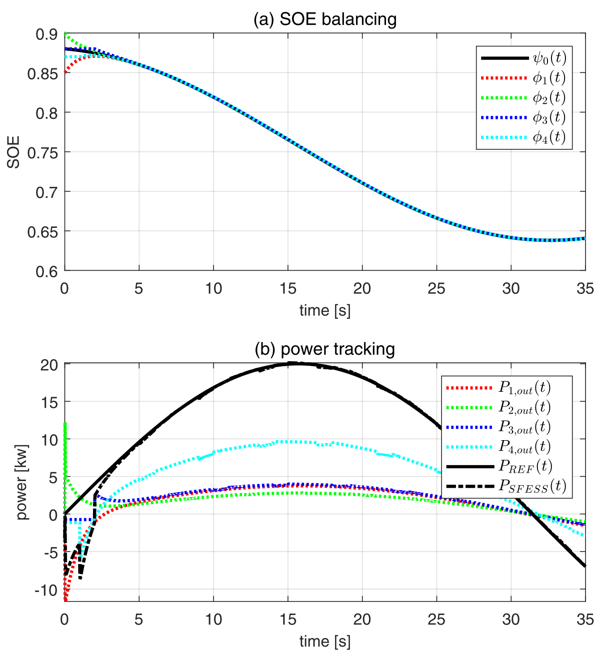

FIGURE 9. System performance for the case of time delay ranged in [0, 0.04]s.

respectively. It can be found that the intermittency of the switching communication network only has effect on the transient response of the system performance and barely has any effect on the system performance when the system enters steady state. The reason lies in that each flywheel system is embedded with both the models of the command generator and the external model. As a result, the steady state can be maintained as long as no additional change is further imposed on the system even if the communication is severely intermittent.

D. EFFECT OF THE TIME DELAY OF THE SWITCHING COMMUNICATION NETWORK ON SYSTEM PERFORMANCE

In this case, we check the effect of the time delay of the switching communication network on system performance. In contrast to the standard case where there is no time delay, we test two scenarios where the time delay between neighboring flywheel systems is ranged in [0, 0.04]s and [0, 0.4]s. The simulation results are shown by Figs. 9 and 10, respectively. It can be observed that as the time delay increases,

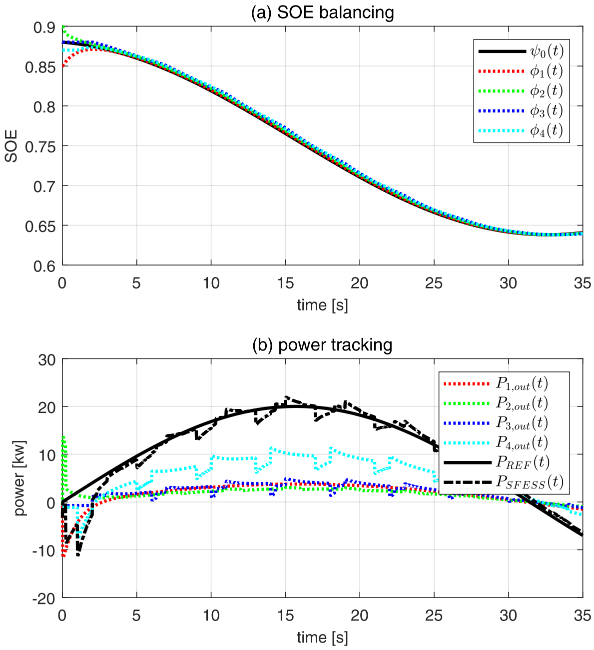

FIGURE 10. System performance for the case of time delay ranged in [0, 0.4]s.

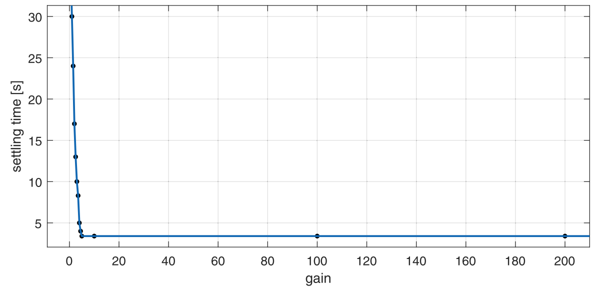

FIGURE 11. Settling time vs. gains μ's for the case of $\kappa = 1$.

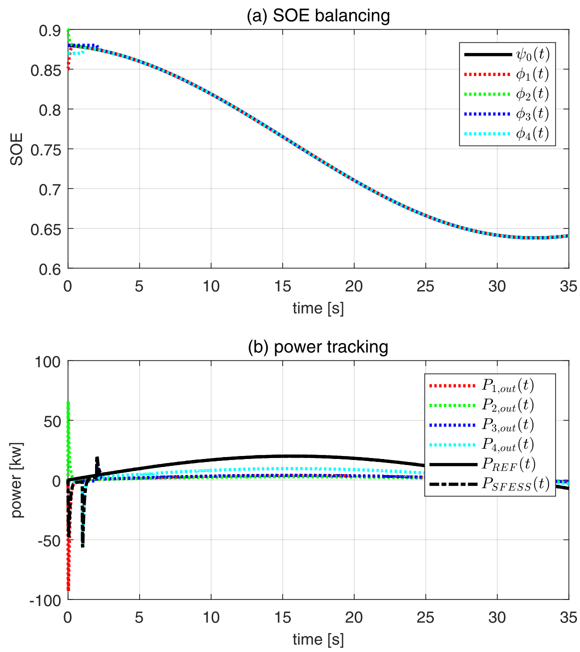

FIGURE 12. System performance for the case of $\kappa = 10$ and $\mu_S = \mu_C = \mu_\eta = \mu_\alpha = \mu_\beta = \mu_\psi = 100$.

the system performance degenerates gradually. Nevertheless, for the case of the time delay ranged in [0, 0.04]s, the system performance is still acceptable. Note that in practice, the time delay for normal transmission lines is usually on the order of 0.5μs per 100 m, and thus if the geographical locations of the flywheel systems of the FESMS are not drastically far away from each other, the time delay of the switching communication network will barely affect system performance.

E. EFFECT OF THE CONTROL GAINS ON SYSTEM PERFORMANCE

In this case, we check the effect of the control gains on system performance. The control gains can be divided into two groups. The first group consists of μ_S, μ_C, μ_η, μ_α, μ_β, μ_ψ, and the second group includes κ only. Due to the cascaded structure of the closed-loop system, the first group of control gains will affect the performance of both $P_{REF}(t)$, $\psi_0(t)$ estimation and $\psi_0(t)$ tracking, while the second group will affect the performance of $\psi_0(t)$ tracking solely. First, we fix κ to check the system performance when the gains in the first group vary. Equations (21), (24) and (25) indicate that larger control gains of the first group would lead to faster estimation of $P_{REF}(t)$ and $\psi_0(t)$, and thus faster tracking of $\psi_0(t)$ by equation (27). As in Case A, we let $\kappa = 1$ and the gains in the first group take the same value. The results are shown by Fig. 11. It can be seen that when the gains of μ's are larger than some threshold, there shall be no further reduction on the settling time.

On the contrary, it can be observed from equation (27) that κ involves both the terms $-\kappa\bar{\phi}_i(t)$ and $\kappa\bar{\psi}_i(t)$. As a result, large κ might not guarantee fast tracking. For example, we let $\mu_S = \mu_C = \mu_\eta = \mu_\alpha = \mu_\beta = \mu_\psi = 100$ and $\kappa = 10$. The simulation result is shown by Fig. 12. In comparison with Case A, it can be seen that the settling time is barely reduced, but the overshoot is much bigger.

In general, due to complex system configuration and different initial conditions, it might not be easy, if possible, to give a systematic approach for gain selection. Instead, the gains might be determined by trial and error in a virtual way before practical implementation.

F. EFFECT OF THE OUTPUT SATURATION ON SYSTEM PERFORMANCE

In practice, the power outputs of the flywheels are subject to limits. In this case, we check the effect of the output saturation on system performance. To show the effect of the output saturation, we adopt the same control gains as in Case E. Suppose the power outputs of all the flywheel systems are limited to 12kw. The simulation result is shown by Fig. 13, which indicates that the output saturation can be directly

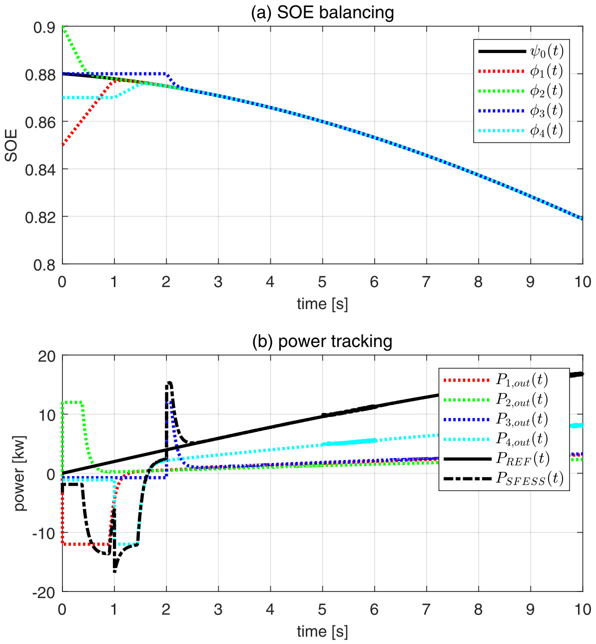

FIGURE 13. System performance for the case of output saturation of 12kw under the control gains $\mu_S = \mu_C = \mu_\eta = \mu_\alpha = \mu_\beta = \mu_\psi = 100$ and $\kappa = 10$.

imposed on the proposed control scheme without any further adjustment.

VI. CONCLUSION

For a heterogenous FESMS, a coordination problem aiming at simultaneous reference power tracking and state-of-energy balancing has been considered. It is first revealed that there exists a common time-varying manifold governed by a nonautonomous dynamic system which guarantees the solution to the coordination problem. Then, the coordination problem is converted into two separate problems, namely, the global double layer estimation problem and the local tracking control problem. Finally, a distributed control scheme is synthesized to solve the coordination problem. Comprehensive case studies are provided for control performance evaluation. For a FESMS consisting of four flywheel systems, under jointly connected communication network, the settling time is about 3.5s. The power loss on the transmission lines will reduce the actual power output of the FESMS. When the switching period of the communication graphs is reset to 0.1s and 2s, the settling time becomes approximately 3s and 7s, respectively. For small time delay within 0.04s, the system performance can be roughly maintained, while for large time delay up to 0.4s, the system performance start to deteriorate. Numerical results show that when the control gains for the augmented command generator estimators are bigger than some threshold, they will barely affect the system settling time. While, the effect of the control gain for the local tracking controller on the system settling time is indecisive. Finally, when adding saturation on the power output of the flywheels, the settling time is about 2.5s, which is similar to that of the case without the saturation constraint, but the overshoot is much smaller.

APPENDIX A
FLYWHEEL SYSTEM MODELING

The electrical and mechanical models of the PMSM/G are as follows[3]:

$$\lambda_q(t) = L_q i_q(t) \tag{29a}$$
$$\lambda_d(t) = L_d i_d(t) + \lambda_f \tag{29b}$$
$$I\dot{\omega}(t) = -B_v\omega(t) + T_e(t) - T_l(t) \tag{29c}$$
$$T_e(t) = 7\frac{3}{2}p(\lambda_f i_q(t) + (L_d - L_q)i_q(t)i_d(t)) \tag{29d}$$

where the subscripts d and q represent the d-axis and q-axis components of a variable in the rotor reference frame under the Park transformation. $i_d(t)$ and $i_q(t)$ are stator currents. L_d and L_q are inductances. λ_f is the PM flux linkage and is considered on the d-axis. I is the inertia of the rotor. B_v is the friction constant. $\omega(t)$ is the rotor angular velocity. $T_e(t)$ and $T_l(t)$ are electrical and load torque, respectively. p is the number of the pole pairs. As in [6], [7], $i_d(t)$ is set to zero and $i_q(t)$ is taken as the reference input. Thus, by letting

$$T(t) = \frac{3}{2}p\lambda_f i_q(t) - T_l(t), \tag{30}$$

the rotor dynamics become:

$$I\dot{\omega}(t) = -B_v\omega(t) + T(t). \tag{31}$$

The kinematic energy stored in the flywheel is

$$E(t) = \frac{1}{2}I\omega(t)^2. \tag{32}$$

Let

$$P(t) = -\dot{E}(t). \tag{33}$$

Then it follows that

$$P(t) = -I\omega(t)\dot{\omega}(t) = B_v\omega(t)^2 - T(t)\omega(t) \tag{34}$$

where the first part $B_v\omega(t)^2 \triangleq P_{loss}(t)$ denotes the power loss due to friction, and the second part $-T(t)\omega(t) \triangleq P_{out}(t)$ denotes the net power output of the flywheel system.

Let $\omega_{\max}$ denote the maximum admissible angular velocity of the flywheel. Then the energy capacity of the flywheel is given by

$$E_{\max} = \frac{1}{2}I\omega_{\max}^2. \tag{35}$$

Thus, the SOE of the flywheel is given by

$$\phi(t) = \frac{E(t)}{E_{\max}} = \frac{\omega(t)^2}{\omega_{\max}^2} = \gamma\omega(t)^2 \tag{36}$$

where $\gamma = 1/\omega_{\max}^2$.

Finally, by (31), (34) and (36), it follows that

$$\begin{aligned}\dot{\phi}(t) &= \frac{2\gamma}{I}(-B_v\omega(t)^2 + T(t)\omega(t)) \\ &= -\frac{2B_v}{I}\gamma\omega(t)^2 + \frac{2\gamma}{I}T(t)\omega(t) \\ &= -\frac{2B_v}{I}\phi(t) - \frac{2\gamma}{I}P_{out}(t). \end{aligned} \tag{37}$$

[3]The models are tested by experimental studies in [6], [7], and the readers may check these references for more details.

REFERENCES

[1] M. Amiryar and K. Pullen, "A review of flywheel energy storage system technologies and their applications," *Appl. Sci.*, vol. 7, no. 3, p. 286, Mar. 2017.
[2] A. A. K. Arani, H. Karami, G. B. Gharehpetian, and M. S. A. Hejazi, "Review of flywheel energy storage systems structures and applications in power systems and microgrids," *Renew. Sustain. Energy Rev.*, vol. 69, pp. 9–18, Mar. 2017.
[3] S. M. Mousavi, F. Faraji, A. Majazi, and K. Al-Haddad, "A comprehensive review of flywheel energy storage system technology," *Renew. Sustain. Energy Rev.*, vol. 67, pp. 477–490, Jan. 2017.
[4] M. Faisal, M. A. Hannan, P. J. Ker, A. Hussain, M. B. Mansor, and F. Blaabjerg, "Review of energy storage system technologies in microgrid applications: Issues and challenges," *IEEE Access*, vol. 6, pp. 35143–35164, May 2018.
[5] X. Chang, Y. Li, W. Zhang, N. Wang, and W. Xue, "Active disturbance rejection control for a flywheel energy storage system," *IEEE Trans. Ind. Electron.*, vol. 62, no. 2, pp. 991–1001, Feb. 2015.
[6] X. Zhang and J. Yang, "A robust flywheel energy storage system discharge strategy for wide speed range operation," *IEEE Trans. Ind. Electron.*, vol. 64, no. 10, pp. 7862–7873, Oct. 2017.
[7] M. Ghanaatian and S. Lotfifard, "Control of flywheel energy storage systems in the presence of uncertainties," *IEEE Trans. Sustain. Energy*, vol. 10, no. 1, pp. 36–45, Jan. 2019.
[8] L. Gong, M. Wang, and C. Zhu, "Immersion and invariance manifold adaptive control of the DC-link voltage in flywheel energy storage system discharge," *IEEE Access*, vol. 8, pp. 144489–144502, Jul. 2020.
[9] J. Lai, Y. Song, and X. Du, "Hierarchical coordinated control of flywheel energy storage matrix systems for wind farms," *IEEE/ASME Trans. Mechatronics*, vol. 23, no. 1, pp. 48–56, Feb. 2018.
[10] Q. Cao, Y.-D. Song, J. M. Guerrero, and S. Tian, "Coordinated control for flywheel energy storage matrix systems for wind farm based on charging/discharging ratio consensus algorithms," *IEEE Trans. Smart Grid*, vol. 7, no. 3, pp. 1259–1267, May 2016.
[11] Y. Sun, J. Hu, and J. Liu, "Periodic event-triggered control of flywheel energy storage matrix systems for wind farms," *IET Control Theory Appl.*, vol. 14, no. 11, pp. 1467–1477, Jul. 2020.
[12] H. Cai and G. Hu, "Distributed control scheme for package-level state-of-charge balancing of grid-connected battery energy storage system," *IEEE Trans. Ind. Informat.*, vol. 12, no. 5, pp. 1919–1929, Oct. 2016.
[13] C. Li, E. A. A. Coelho, T. Dragicevic, J. M. Guerrero, and J. C. Vasquez, "Multiagent-based distributed state of charge balancing control for distributed energy storage units in AC microgrids," *IEEE Trans. Ind. Appl.*, vol. 53, no. 3, pp. 2369–2381, May 2017.
[14] H. Cai, "Power tracking and state-of-energy balancing of an energy storage system by distributed control," *IEEE Access*, vol. 8, pp. 170261–170270, Sep. 2020.
[15] T. Morstyn, B. Hredzak, and V. G. Agelidis, "Distributed cooperative control of microgrid storage," *IEEE Trans. Power Syst.*, vol. 30, no. 5, pp. 2780–2789, Sep. 2015.
[16] T. Liu and J. Huang, "Leader-following consensus with disturbance rejection for uncertain Euler–Lagrange systems over switching networks," *Int. J. Robust Nonlinear Control*, vol. 29, no. 18, pp. 6638–6656, Oct. 2019.
[17] Y. Su and J. Huang, "Cooperative output regulation with application to multi-agent consensus under switching network," *IEEE Trans. Syst., Man, Cybern., B, Cybern.*, vol. 42, no. 3, pp. 864–875, Jun. 2012.
[18] X. Dong and G. Hu, "Time-varying formation control for general linear multi-agent systems with switching directed topologies," *Automatica*, vol. 73, pp. 47–55, Nov. 2016.
[19] X. Dong, Y. Zhou, Z. Ren, and Y. Zhong, "Time-varying formation tracking for second-order multi-agent systems subjected to switching topologies with application to quadrotor formation flying," *IEEE Trans. Ind. Electron.*, vol. 64, no. 6, pp. 5014–5024, Jun. 2017.
[20] H. Cai and G. Hu, "Distributed robust hierarchical power sharing control of grid-connected spatially concentrated AC microgrid," *IEEE Trans. Control Syst. Technol.*, vol. 27, no. 3, pp. 1012–1022, May 2019.

HAIMING LIU received the B.Eng., M.Eng., and Ph.D. degrees in automation from the South China University of Technology, Guangzhou, China, in 2000, 2003, and 2010, respectively. Since 2003, he has been a Full Lecturer and a Senior Engineer with the School of Automation Science and Engineering, South China University of Technology. His research interests include cluster control of multi-agent systems and its applications in unmanned robot cluster and smart grid.

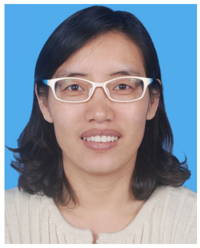

HUANLI GAO received the B.S. and M.S. degrees from Shandong University, Jinan, China, in 2002 and 2005, respectively, and the Ph.D. degree from the South China University of Technology, Guangzhou, China, in 2008. From October 2007 to April 2008, she received national support to study at the School of Electrical and Electronic Engineering, Nanyang Technological University, Singapore. She is currently working with the School of Automation Science and Engineering, South China University of Technology. Her current research interests include autonomous vehicle control, cooperative control, and networked control systems.

SHUPING GUO received the B.Eng. degree in automation from the Tianjin University of Technology, Tianjin, China, in 2019. He is currently pursuing the M.Eng. degree in control science and engineering with the South China University of Technology, Guangzhou, China. His current research interests include cyber-physical systems and smart grid.

HE CAI (Member, IEEE) received the B.Eng. degree in automation from the University of Science and Technology of China, Hefei, China, in 2010, and the Ph.D. degree in mechanical and automation engineering from The Chinese University of Hong Kong, Hong Kong, in 2014. From 2014 to 2017, he worked as a Research Fellow with the School of Electrical and Electronic Engineering, Nanyang Technological University, Singapore. Since 2017, he has been a Full Professor with the School of Automation Science and Engineering, South China University of Technology, Guangzhou, China. His research interests include cooperative control of multiagent systems and its applications in intelligent robots and smart grid.